Ab Initio Anharmonic Force Field and Rotational Analyses of Infrared Bands of Perchloryl Fluoride

Elisabetta Cané, Luciano Fusina,* Manuele Lamarra, Riccardo Tarroni, and Klaus Burczyk†

Dipartimento di Chimica Fisica e Inorganica, Facoltà di Chimica Industriale, Università di Bologna, Viale Risorgimento 4, 40136 Bologna, Italy

Received: July 29, 2008; Revised Manuscript Received: October 2, 2008

Perchloryl fluoride, $FClO_3$, has been studied both experimentally and theoretically, using high-resolution Fourier transform spectroscopy and high-level ab initio methods. The geometry, dipole moment, and anharmonic force field of the molecule have been calculated ab initio, using the coupled-cluster with single, double, and perturbative triple excitations [CCSD(T)] level of theory. The infrared spectra of monoisotopic species have been recorded. The $\nu_1 + \nu_2$ bands of $F^{35}Cl^{16}O_3$, $F^{37}Cl^{16}O_3$, $F^{35}Cl^{18}O_3$, and $F^{37}Cl^{18}O_3$, the $\nu_2 + \nu_3$ and $\nu_2 + \nu_3 - \nu_3$ bands of $F^{35}Cl^{16}O_3$ and $F^{37}Cl^{16}O_3$, and the $2\nu_3 - \nu_3$ band of $F^{37}Cl^{16}O_3$ have been analyzed. The spectroscopic parameters obtained from these and from previous analyses have been compared with the theoretical results.

1. Introduction

Perchloryl fluoride is a chemically stable prolate symmetric rotor with a very pronounced quasi-spherical character, which has been extensively studied using high-resolution spectroscopic techniques.[1−14] Conversely, theoretical studies are essentially lacking, if one excludes the harmonic force field of the molecule.[6,15] This is quite surprising, because in general experimental progress stimulates theoretical work (and vice versa) as pointed out in a recent review on this topic.[16] Moreover, some challenging problems related to $FClO_3$ derive essentially from the hypervalent character of the Cl atom, the very small molecular dipole moment, and the unusual isotopic dependence of few band intensities.[8,17] All these issues, together with the wealth of highly accurate spectroscopic parameters for several isotopically substituted species, prompted us to perform the ab initio calculation of a quartic anharmonic force field.

$FClO_3$ is a molecule of C_{3v} symmetry with six normal modes of vibration, ν_1, ν_2, and ν_3 of a_1 symmetry and ν_4, ν_5, and ν_6 of e symmetry. Four monoisotopic species, $F^{35}Cl^{16}O_3$, $F^{37}Cl^{16}O_3$, $F^{35}Cl^{18}O_3$, and $F^{37}Cl^{18}O_3$, have been synthesized[7] to avoid the spectral congestion due to the presence of $^{35/37}Cl$ isotopes in the natural abundance ratio 75/25 in the sample. The high-resolution infrared spectra of the monoisotopic samples have been recorded from 450 to 2000 cm^{-1}.[7] Up to now the ground state and all fundamental bands of the four symmetric species have been analyzed, so the molecular constants of the ground and of the $v_i = 1$, with $i = 1, 2, ..., 6$, excited states have been obtained.[1−5,7−9,11,13] All fundamentals do not show any perturbation due to interactions with nearby vibration states except ν_4. In fact the $v_4 = 1$ state interacts significantly with the $v_2 = v_5 = 1$ state through a Fermi-type resonance.[4,11,13] The vibration−rotation interaction parameters α_i^A and α_i^B with $i = 1, 2, ..., 6$, and the equilibrium molecular constants A_e and B_e have been calculated from these spectroscopic data.[11,13] The equilibrium geometry of the molecule has also been determined, $r_e(ClO) = 139.7(3)$ pm, $r_e(ClF) = 161.0(5)$ pm, and $\angle(OClO) = 115.7(4)°$.[13] In addition, the $2\nu_1$, $2\nu_2$, $2\nu_3$, $2\nu_5$, and $2\nu_6$ overtone bands,[10,12,14] the $\nu_2 + \nu_5$ combination bands,[4,11,13] and the $\nu_1 + \nu_3 - \nu_3$ hot bands[8] have been rotationally analyzed. By combining their band origins with those of the fundamentals, the x_{ij} and g_{ii} anharmonicity constants have been derived.

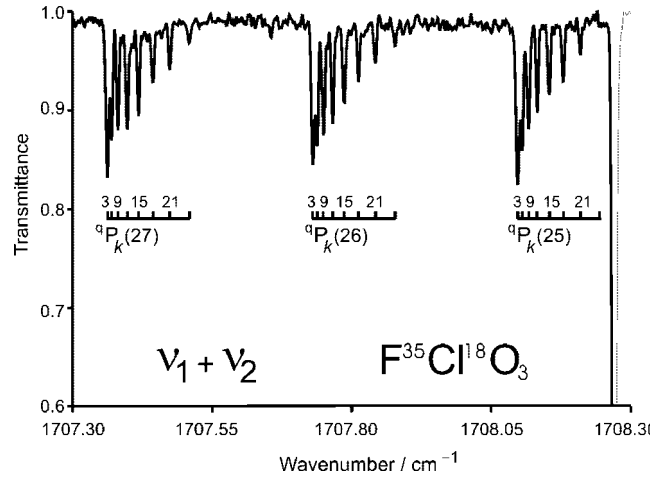

Figure 1. Detail of the $\nu_1 + \nu_2$ band of $F^{35}Cl^{18}O_3$ in the region of $^qP_k(J)$ branches. The J and K quantum number values are indicated. The very strong line on the right of the figure is due to H_2O.

In this investigation we use high-level ab initio methods to compute, for the first time, the full quartic anharmonic force field of perchloryl fluoride. The theoretical force field is then used to evaluate the anharmonicity and the vibration−rotation interaction constants. The rotational analyses of the $\nu_1 + \nu_2$ and $\nu_2 + \nu_3$ combination bands are presented from high-resolution spectra of monoisotopic samples. The weak $\nu_1 + \nu_2$ parallel bands are observed in the range of 1680−1800 cm^{-1} for the four isotopologues. The $\nu_2 + \nu_3$ parallel bands of medium intensity are observed from 1220 to 1300 cm^{-1}. They have been analyzed only in the spectra of $F^{35}Cl^{16}O_3$ and $F^{37}Cl^{16}O_3$ where they are not overlapped by the strong ν_4 bands. In addition,

* Corresponding author. Phone: +390512093707. Fax: +390512093690. E-mail: fusina@ms.fci.unibo.it.

† Present address: Anorganische Chemie, FB C Universität, 42097 Wuppertal, Germany.

10.1021/jp806710q CCC: $40.75
Published on Web 11/21/2008

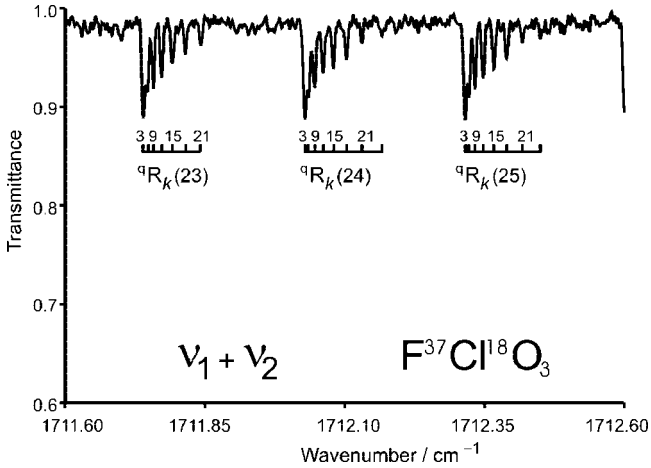

Figure 2. Detail of the $\nu_1 + \nu_2$ band of $F^{37}Cl^{18}O_3$ in the region of ${}^qR_k(J)$ branches. The J and K quantum number values are indicated.

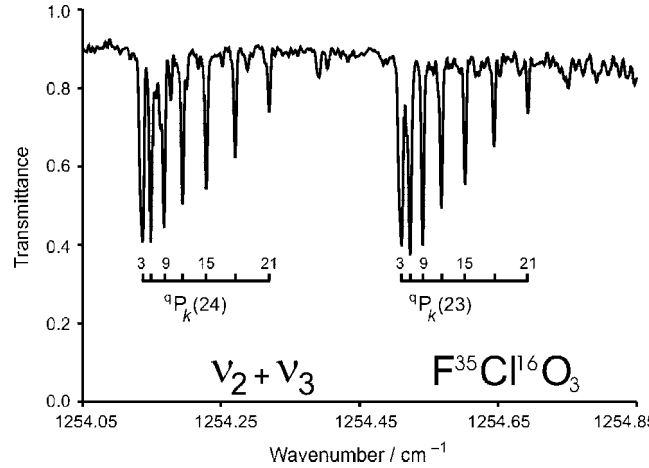

Figure 3. Detail of the $\nu_2 + \nu_3$ band of $F^{35}Cl^{16}O_3$ in the region of ${}^qP_k(J)$ branches. The J and K quantum number values are indicated.

three parallel hot bands are presented: the $\nu_2 + \nu_3 - \nu_3$ of $F^{35}Cl^{16}O_3$ and $F^{37}Cl^{16}O_3$, observed at about 700 cm^{-1} in the region of the ν_2 fundamental, and the $2\nu_3 - \nu_3$ of $F^{37}Cl^{16}O_3$, at 550 cm^{-1}, in the region of ν_3. The x_{12} and x_{23} anharmonicity constants are derived for the first time from the band origins of the combination and hot bands. All the experimental values of the molecular parameters determined in this work or previously reported in the literature are compared to those calculated from the ab initio force field.

Hereafter, the four species $F^{35}Cl^{16}O_3$, $F^{37}Cl^{16}O_3$, $F^{35}Cl^{18}O_3$, and $F^{37}Cl^{18}O_3$ will be indicated with the short notation (35,16), (37,16), (35,18), and (37,18).

2. Computational Details

To our knowledge, only the theoretical harmonic force field of $FClO_3$ has been proposed.[6,15] In this work we applied state-of-the-art ab initio methodologies to obtain its quartic force field. All calculations have been performed with the Aces II suite of quantum chemistry programs, Mainz−Austin−Budapest version.[18]

The ground-state equilibrium geometries and dipole moments have been calculated at second-order Møller−Plesset perturbation (MP2)[19] and at the coupled-cluster with single, double, and perturbative triple excitations [CCSD(T)][20] levels of theory with the cc-pVTZ,[21] cc-pVQZ,[21] cc-pV(T+d)Z,[22] cc-pV(Q+d)Z,[22] and cc-pCVTZ[23] basis sets. By comparison with the corresponding experimental values, the CCSD(T) method and the cc-pCVTZ basis have been chosen for the calculation of the Hessian, as being the best compromise between accuracy and computational speed.

The analytical Hessian[24] has been then calculated with the cc-pCVTZ basis, including core correlation at the corresponding theoretical equilibrium geometry. The full cubic and quartic force fields in Cartesian coordinates were subsequently computed from the finite differences of the analytical Hessians obtained at a lower level of theory, that is, MP2 with the cc-pVTZ basis sets[21] and within the frozen core approximation. Such a hybrid approach relies on the smaller effects of basis size and electron correlation on the cubic and quartic force fields.[25] The displaced Cartesian geometries, with a step size of 0.006 bohr, have been generated starting from the CCSD(T)/cc-pCVTZ equilibrium structure. The numerical stability of the procedure against the step size was checked by comparing[26] the values of the F_{ijkl} and F_{klij} quartic force field elements in

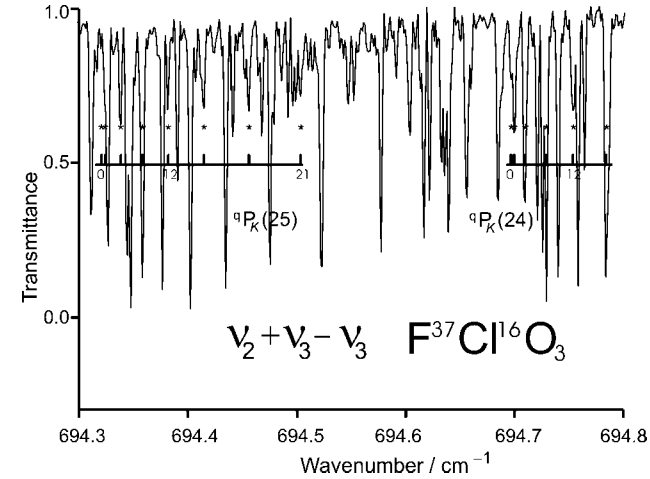

Figure 4. Detail of the $\nu_2 + \nu_3 - \nu_3$ hot band of $F^{37}Cl^{16}O_3$ in the region of ${}^qP_k(J)$ branches. The J and K quantum number values are indicated. The assigned lines have been evidenced with a star. The stronger lines in the figure belong to the ${}^qP_k(J)$ branches of ν_2 band. Their assignments are not indicated to avoid congestion.

Cartesian coordinates. The maximum absolute difference was 0.027 aJ·Å^{-4}.

The transformation of force constants from Cartesian to normal coordinates and the computation of the spectroscopic constants[27] have been performed with the SPECTRO program,[28] and the transformation to symmetry internal coordinates was performed with the INTDER program.[25,29,30]

3. Experimental Section

The syntheses of the monoisotopic samples have been already reported.[7] In the same paper the experimental conditions for the recording of Fourier transform infrared (FTIR) spectra are also listed in Tables 1 and 2 for $FCl^{16}O_3$ and $FCl^{18}O_3$ species, respectively. The present analyses are based on the spectra recorded at that time at room temperature. The spectra of columns V and VI, in Table 1 have been used for both $\nu_1 + \nu_2$ and $\nu_2 + \nu_3$ of (37,16) and (35,16), respectively, spectra I and III for $\nu_2 + \nu_3 - \nu_3$ and $2\nu_3 - \nu_3$ of (37,16), respectively, and spectrum XII for $\nu_2 + \nu_3 - \nu_3$ of (35,16). The $\nu_1 + \nu_2$ bands of (35,18) and (37,18) are from spectra of columns M and L in Table 2, respectively. The spectral resolution is 4.4×10^{-3} cm^{-1} (spectra V, VI, L, and M), 2.8×10^{-3} cm^{-1} (spectrum I), 5.5

TABLE 1: Ground-State Molecular Constants (cm^{-1}) of $FClO_3$[a]

parameter	$F^{35}Cl^{16}O_3$	$F^{37}Cl^{16}O_3$	$F^{35}Cl^{18}O_3$	$F^{37}Cl^{18}O_3$
$A_0 \times 10^1$	1.871217(42)	1.871364(29)	1.66325417(100)	1.66331592(59)
$B_0 \times 10^1$	1.7541085(8)	1.7532656(6)	1.6379784(5)	1.6374819(4)
$D_{0J} \times 10^8$	4.9979(9)	4.9939(9)	4.2716(7)	4.265 4(7)
$D_{0JK} \times 10^8$	5.534(5)	5.591(6)	3.937(4)	3.977(4)
$D_{0K} \times 10^8$	−7.6	−7.6	−5.91599(142)	−6.28844(104)
$\varepsilon_0 \times 10^9$	−3.07(60)	−3.20(64)	−5.31(8)	−5.47(9)

[a] From Table 4 of ref 7. Standard uncertainties (1σ) in parentheses refer to the least significant digits.

TABLE 2: Molecular Constants (cm^{-1}) of $FClO_3$ in the $v_1 = v_2 = 1$ Excited States[a]

parameter	$F^{35}Cl^{16}O_3$	$F^{37}Cl^{16}O_3$	$F^{35}Cl^{18}O_3$	$F^{37}Cl^{18}O_3$
E_v^0	1777.351013(76)	1764.767874(73)	1716.763290(42)	1704.351432(43)
$A \times 10^1$	1.8648697(15)	1.8650214(15)	1.65785444(88)	1.65791746(88)
$B \times 10^1$	1.7460073(13)	1.7454155(10)	1.63002047(47)	1.62968765(54)
$D_J \times 10^8$	4.8949(43)	4.9359(28)	4.2307(11)	4.2149(14)
$D_{JK} \times 10^8$	5.8189(98)	5.7807(74)	4.1086(38)	4.1540(44)
$D_K \times 10^8$	−7.8124(78)	−7.7621(78)	−6.0454(41)	−6.4005(38)
no. of assigned/fitted transitions	1102/1092	1255/1239	1427/1422	1357/1357
J'_{max}/K'_{max}	61/57	61/57	69/60	67/60
standard deviation of the fit	0.00069	0.00060	0.00047	0.00048

[a] Standard uncertainties (1σ) in parentheses refer to the least significant digits.

TABLE 3: Molecular Constants (cm^{-1}) of $FCl^{16}O_3$ in the $v_2 = v_3 = 1$ Excited States[a]

parameter	$F^{35}Cl^{16}O_3$	$F^{37}Cl^{16}O_3$
E_v^0	1262.833508(27)	1252.553653(31)
$A \times 10^1$	1.87031559(68)	1.87047357(84)
$B \times 10^1$	1.74900997(23)	1.74831173(29)
$D_J \times 10^8$	5.05388(38)	5.03858(53)
$D_{JK} \times 10^8$	5.5350(15)	5.6124(20)
$D_K \times 10^8$	−7.6359(33)	−7.6326(51)
no. of assigned/fitted transitions	1320/1313	1053/1035
J'_{max}/K'_{max}	84/48	79/45
standard deviation of the fit	0.00037	0.00037

[a] Standard uncertainties (1σ) in parentheses refer to the least significant digits.

$\times 10^{-3}$ cm^{-1} (spectrum III), and 3.3×10^{-3} cm^{-1} (spectrum XII). The wavenumber precision has been estimated to be 1.5×10^{-4} cm^{-1} for spectrum I, 2.0×10^{-4} cm^{-1} for spectra XII, L, and M, and 3.0×10^{-4} cm^{-1} for spectra III, V, and VI.

4. Spectra Description

The shape of $\nu_1 + \nu_2$ parallel band is very similar in the four isotopologues. It is a weak band with the quite dense absorption maximum of the ${}^qQ_k(J)$ branches that spread over about 3 cm^{-1} and is centered at 1777 cm^{-1} in (35,16), 1765 cm^{-1} in (37,16), 1717 cm^{-1} in (35,18), and 1704 cm^{-1} in (37,18). The J structure of the Q branch degrades to lower wavenumbers. The K-structures of the ${}^qP_k(J)$ and ${}^qR_k(J)$ subbranches are resolved except for the $K = 0$ and 3 transitions and degrade to higher wavenumbers with increasing K values (see Figures 1 and 2). As it is evident by inspection of Figures 1 and 2 only the transitions with $K = 3p$, with $p = 0, 1, 2, ...$, are observed. In fact, the levels with $K \neq 3p$ have statistical weight equal to zero as both the ^{16}O and ^{18}O atoms have nuclear spin quantum number $I = 0$. The $\nu_1 + \nu_2$ bands are unperturbed in the four isotopologues.

The unperturbed $\nu_2 + \nu_3$ parallel bands of (35,16) and (37,16) of medium intensity are centered at about 1263 and 1253 cm^{-1}, respectively. Since they are close to the strong perpendicular bands of the ν_4 fundamentals, centered at about 1317 and 1302 cm^{-1} in (35,16) and (37,16), the ${}^qR_k(J)$ subbranches at higher wavenumbers are overlapped by ν_4. The overall band shape is almost the same in (35,16) and (37,16) and very similar to that of $\nu_1 + \nu_2$ (see Figure 3).

The $\nu_2 + \nu_3 - \nu_3$ hot bands of (35,16) and (37,16) have been observed in the region of the ν_2 fundamentals, at about 713 and 703 cm^{-1}, respectively. They are parallel bands of medium-weak intensity. Thanks to a careful check of the observed transitions it has been possible to distinguish those belonging to the $\nu_2 + \nu_3 - \nu_3$ hot band from the stronger ones of ν_2 (see Figure 4).

TABLE 4: Molecular Constants (cm^{-1}) for the $\nu_2 + \nu_3 - \nu_3$ and $2\nu_3 - \nu_3$ Hot Bands of $FCl^{16}O_3$[a]

	$F^{35}Cl^{16}O_3$		$F^{37}Cl^{16}O_3$		
parameter	$\nu_2 + \nu_3 - \nu_3$	ν_3[b]	$\nu_2 + \nu_3 - \nu_3$	$2\nu_3 - \nu_3$	ν_3[b]
E_v^0	712.953772(40)	549.87956(8)	703.364251(40)	547.88188(20)	549.18943(8)
$A \times 10^1$	1.8703215(12)	1.870929(42)	1.8704746(17)	1.8700841(20)	1.871092(29)
$B \times 10^1$	1.74901126(64)	1.7538448(14)	1.74830833(65)	1.7525739(37)	1.7529569(11)
$D_J \times 10^8$	5.0516(21)	5.1744(34)	5.0228(22)	5.3343(84)	5.1623(26)
$D_{JK} \times 10^8$	5.6340(72)	5.295(14)	5.6646(88)	5.2966[c]	5.2966(97)
$D_K \times 10^8$	−7.7330(55)	−7.51(10)	−7.745(17)	−7.48[c]	−7.48(10)
no. of assigned/fitted transitions	940/921		709/709	71/70	
J'_{max}/K'_{max}	58/54		55/36	65/15	
standard deviation of the fit	0.00034		0.00036	0.00051	

[a] Standard uncertainties (1σ) in parentheses refer to the least significant digits. [b] From Table 3 of ref 8. [c] Fixed to the value of the corresponding constant in the $v_3 = 1$ state.

TABLE 5: Comparison between Theoretical and Experimental Geometries and Dipole Moments for $FClO_3$

	r_e(ClO)/pm	r_e(ClF)/pm	∠(OClO)/deg	∠(FClO)/deg	dipole moment/debye
MP2/cc-pVTZ	141.77	164.83	115.90	101.85	−0.1059
MP2/cc-pV(T+d)Z	140.35	162.64	115.84	101.94	−0.0605
MP2/cc-pCVTZ	140.19	162.41	115.83	101.95	−0.0578
CCSD(T)/cc-pVTZ	142.20	163.22	115.72	102.11	−0.0058
CCSD(T)/cc-pV(T+d)Z	140.59	161.28	115.68	102.16	+0.0244
CCSD(T)/cc-pCVTZ	140.38	161.06	115.68	102.17	+0.0254
MP2/cc-pVQZ	140.80	163.58	115.86	101.90	−0.0755
MP2/cc-pV(Q+d)Z	140.01	162.28	115.82	101.96	−0.0488
CCSD(T)/cc-pVQZ	141.05	161.93	115.69	102.16	+0.0179
CCSD(T)/cc-pV(Q+d)Z	140.17	160.79	115.66	102.20	+0.0356
experimental	139.7(3)[a]	161.0(5)[a]	115.7(4)[a]	102.0(8)[a]	0.02700[b]

[a] From ref 13. Standard uncertainties (1σ) in parentheses refer to the least significant digits. [b] Absolute value from ref 2.

TABLE 6: Definition of Symmetry Coordinates for $FClO_3$[a]

	definition[b]
S_1	$(\Delta r_1 + \Delta r_2 + \Delta r_3)/\sqrt{3}$
S_{2a}	$(\Delta\alpha_1 + \Delta\alpha_2 + \Delta\alpha_3 - \Delta\beta_1 - \Delta\beta_2 - \Delta\beta_3)/\sqrt{6}$
S_{2b}	$(\Delta\alpha_1 + \Delta\alpha_2 + \Delta\alpha_3 + \Delta\beta_1 + \Delta\beta_2 + \Delta\beta_3)/\sqrt{6}$
S_2*[c]	$PS_{2a} - QS_{2b} = -0.47609812(\Delta\beta_1 + \Delta\beta_2 + \Delta\beta_3)$ $+0.32659442(\Delta\alpha_1 + \Delta\alpha_2 + \Delta\alpha_3)$
S_3	ΔR
S_{4a}	$(2\Delta r_1 - \Delta r_2 - \Delta r_3)/\sqrt{6}$
S_{4b}	$(\Delta r_2 - \Delta r_3)/\sqrt{2}$
S_{5a}	$(2\Delta\alpha_1 - \Delta\alpha_2 - \Delta\alpha_3)/\sqrt{6}$
S_{5b}	$(\Delta\alpha_2 - \Delta\alpha_3)/\sqrt{2}$
S_{6a}	$(2\Delta\beta_1 - \Delta\beta_2 - \Delta\beta_3)/\sqrt{6}$
S_{6b}	$(\Delta\beta_2 - \Delta\beta_3)/\sqrt{2}$

[a] According to ref 31. [b] $r = r_{ClO}$, $R = r_{ClF}$, $\alpha = \angle(OClO) = 115.68°$, $\beta = \angle(FClO) = 102.17°$. [c] $P = (1 + K)/(2 + 2K^2)^{1/2}$, $Q = (1 - K)/(2 + 2K^2)^{1/2}$, $K = -3 \sin\beta \cos\beta/\sin\alpha$.

The $2\nu_3 - \nu_3$ hot band of (37,16) at about 548 cm^{-1} is evident in the spectrum of ν_3 illustrated in Figure 1 of ref 8, where the rotational analyses of ν_3 fundamentals of the four isotopologues have been reported. As observed in ν_3[8] and $2\nu_3$,[12] the Q branch is sharp and the *K*-structure of the Q, P, and R branches is not resolved.

5. Analysis

5.1. The $\nu_1 + \nu_2$ and $\nu_2 + \nu_3$ Combination Bands. The lines of the parallel bands have been assigned on the basis of the very precise ground-state combination differences (GSCD), calculated using the ground-state molecular constants[7] listed in Table 1 for completeness. Since the sets contain ε_0, the coefficient of the off-diagonal part of the effective Hamiltonian, becoming important in quasi-spherical tops,[7] the energies of the ground states have been obtained as eigenvalues of the appropriate energy matrices. The diagonal elements have been calculated as

$$E_v(J,k)/hc = E_v^0 + B_v[J(J+1) - k^2] + A_v k^2 - D_{vJ}[J(J+1)]^2 - D_{vJK}[J(J+1)]k^2 - D_{vK}k^4 \quad (1)$$

with $v = 0$, and the off-diagonal ones by

$$\langle J,k|H/hc|J,k\pm3\rangle = \varepsilon_0(2k\pm3)[J(J+1) - k(k\pm1)]^{1/2} \times [J(J+1) - (k\pm1)(k\pm2)]^{1/2} \times [J(J+1) - (k\pm2)(k\pm3)]^{1/2} \quad (2)$$

Since no splitting of the $K = 3$ lines into A_1, A_2 components has been observed, the energies of the $K'' = 3$ levels have been averaged to calculate the transition wavenumbers. The assigned transitions have been fitted to six parameters of the vibrationally excited states, whose energies have been calculated using eq 1. Weights equal to 1.0, 0.1, or 0.0, have been attributed to the experimental wavenumbers, according to the purity of the corresponding lines. The results for the $\nu_1 + \nu_2$ and $\nu_2 + \nu_3$ bands are collected in Tables 2 and 3, respectively. The standard deviations of the fits are very good, being almost equal, or about two times the experimental precisions, for the $\nu_2 + \nu_3$ and $\nu_1 + \nu_2$ analyses, respectively.

5.2. The $\nu_2 + \nu_3 - \nu_3$ and $2\nu_3 - \nu_3$ Hot Bands. The assignments have been done by means of the lower state

TABLE 7: Harmonic Force Field of $FClO_3$ in Symmetry Coordinates and Potential Energy Distribution (PED) of $F^{35}Cl^{16}O_3$[a]

	force constants f_{ij}			PED					
i j	this work	ref 15	ref 6	ν_1	ν_2	ν_3	ν_4	ν_5	ν_6
1 1	10.329	9.90	10.246	95.6	4.4				
1 2	0.180	0.13[b,c]	0.136[b,c]						
1 3	−0.025	0.07[b]	−0.309[b]						
2 2	2.480	2.58[b]	2.477[b]		33.4	64.8			
2 3	−0.553	−0.58[b]	−0.568[c]						
3 3	3.774	3.49[b]	3.628[b]		62.3	35.2			
4 4	10.332	9.69	9.92				95.7	4.1	
4 5	−0.367	−0.29	−0.362						
4 6	0.173	0.33[c]	0.144[c]						
5 5	1.558	1.53	1.559					76.7	20.8
5 6	−0.300	−0.26[c]	−0.307[c]						
6 6	1.553	1.49	1.538					19.2	79.0

[a] Units are in aJ/$Å^{-n}$, where *n* is the number of stretches in the definition of the force constant. Force constants independent or nonzero by symmetry are reported (ref 32). [b] The f_{12}, f_{13}, and f_{22}, f_{33} constants in refs 6, 15 have been interchanged according to the different definition of the symmetry coordinates. [c] The sign of these force constants has been changed because of the sign differences in the definition of the symmetry coordinates in refs 6, 15.

TABLE 8: Cubic Anharmonic Force Field of $FClO_3$[a]

i j k	f_{ijk}	*i j k*	f_{ijk}	*i j k*	f_{ijk}	*i j k*	f_{ijk}
1 1 1	−42.641	1 4 4	−42.607	2 5 6	0.617	4 4 6	0.093
1 1 2	−1.155	1 4 5	1.100	2 6 6	1.634	4 5 5	0.649
1 1 3	−0.274	1 4 6	−0.144	3 4 4	0.406	4 5 6	−0.021
1 2 2	−2.317	1 5 5	−2.121	3 4 5	−0.077	4 6 6	−0.403
1 2 3	1.294	1 5 6	0.161	3 4 6	−1.353	5 5 5	−1.154
1 3 3	−2.522	1 6 6	−1.149	3 5 5	−0.146	5 5 6	−0.290
2 2 2	4.211	2 4 4	−0.410	3 5 6	0.219	5 6 6	0.297
2 2 3	−2.049	2 4 5	0.430	3 6 6	−2.521	6 6 6	−2.117
2 3 3	1.698	2 4 6	1.494	4 4 4	−29.942		
3 3 3	−20.806	2 5 5	−1.562	4 4 5	−0.967		

[a] Units are in aJ/Å^{-n}, where n is the number of stretches in the definition of the force constant.

TABLE 9: Quartic Anharmonic Force Field of $FClO_3$[a]

i j k l	f_{ijkl}	*i j k l*	f_{ijkl}	*i j k l*	f_{ijkl}
1 1 1 1	185.708	2 2 4 5	−1.349	2 5 5 6	0.489
1 1 1 2	6.425	2 2 4 6	0.930	2 5 6 6	−0.388
1 1 1 3	6.113	2 2 5 5	2.316	2 6 6 6	−1.960
1 1 2 2	5.556	2 2 5 6	0.356	3 4 4 4	2.566
1 1 2 3	−1.886	2 2 6 6	4.404	3 4 4 5	0.060
1 1 3 3	0.683	2 3 4 4	−0.435	3 4 4 6	1.039
1 2 2 2	−1.722	2 3 4 5	0.209	3 4 5 5	0.021
1 2 2 3	2.611	2 3 4 6	−2.852	3 4 5 6	0.009
1 2 3 3	−3.799	2 3 5 5	0.176	3 4 6 6	2.384
1 3 3 3	6.465	2 3 5 6	−0.143	3 5 5 5	−0.144
2 2 2 2	21.619	2 3 6 6	−4.038	3 5 5 6	0.214
2 2 2 3	−7.188	3 3 4 4	3.042	3 5 6 6	−0.111
2 2 3 3	4.331	3 3 4 5	−0.074	3 6 6 6	4.019
2 3 3 3	−1.809	3 3 4 6	4.761	4 4 4 4	230.443
3 3 3 3	117.197	3 3 5 5	0.030	4 4 4 5	−1.119
1 1 4 4	162.674	3 3 5 6	0.067	4 4 4 6	3.600
1 1 4 5	−4.530	3 3 6 6	3.767	4 4 5 5	1.910
1 1 4 6	1.120	1 4 4 4	113.528	4 4 5 6	−0.043
1 1 5 5	5.521	1 4 4 5	1.482	4 4 6 6	0.467
1 1 5 6	−0.500	1 4 4 6	1.422	4 5 5 5	−2.540
1 1 6 6	0.372	1 4 5 5	−1.830	4 5 5 6	0.184
1 2 4 4	1.374	1 4 5 6	0.070	4 5 6 6	0.004
1 2 4 5	−1.502	1 4 6 6	0.166	4 6 6 6	2.769
1 2 4 6	−0.647	1 5 5 5	2.207	5 5 5 5	5.130
1 2 5 5	2.222	1 5 5 6	0.227	5 5 5 6	−1.440
1 2 5 6	−0.545	1 5 6 6	−0.274	5 5 6 6	0.795
1 2 6 6	−0.784	1 6 6 6	1.252	5 6 6 6	−1.438
1 3 4 4	4.713	2 4 4 4	0.477	6 6 6 6	8.475
1 3 4 5	−0.389	2 4 4 5	1.110	4a4a5b5b	−1.242
1 3 4 6	0.977	2 4 4 6	−0.273	4a4a5b6b	0.060
1 3 5 5	−0.049	2 4 5 5	−0.699	4a4a6b6b	0.450
1 3 5 6	−0.080	2 4 5 6	0.047	4a5a6b6b	0.059
1 3 6 6	3.248	2 4 6 6	−1.011	4a6a5b6b	0.004
2 2 4 4	0.346	2 5 5 5	0.579	5a5a6b6b	0.489

[a] Units are in aJ/Å^{-n}, where n is the number of stretches in the definition of the force constant.

combination differences (LSCD), calculated from the molecular constants of the $\upsilon_3 = 1$ excited states[8] listed in Table 4 for completeness. The lower and the excited-state energies have been calculated with eq 1, and the assigned transitions have been fitted to six parameters of the excited state. The results are shown in Table 4. The standard deviations of the fits are very good, being about 2 times the spectral precisions.

6. Ab Initio Force Fields

In Table 5 we compare with experiment[2,13] the theoretical geometries and dipole moments, for various combinations of methods and basis sets. The original cc-pVTZ and cc-pVQZ bases for chlorine are clearly not adequate to accurately reproduce the experimental equilibrium geometry, in particular the Cl−F bond. Within the frozen core approximation, the inclusion of tight "d" functions on the chlorine set, as accomplished in the cc-pV(T+d)Z and cc-pV(q+d)Z sets,[22] is required to shorten the Cl−F bond toward the experimental value. The MP2 method is unable to predict this bond length accurately, even with large basis sets. Conversely, the values of the Cl−O internuclear distance and of the ∠(OClO) angle are closer to experiment and less sensitive to the combination of basis and method.

The value of the dipole moment is always predicted to be very small, and its sign is closely related to the ∠(OClO) angle, being positive, i.e., pointing to the fluorine atom, for smaller value of the angle.

The definition of symmetry internal coordinates is reported in Table 6 and strictly follows the prescriptions of King et al.[31] This choice requires a careful comparison with previously published harmonic force fields,[6,15] because the S_2 and S_3 symmetry coordinates are interchanged and the signs of S_{4a}, S_{4b}, S_{5a}, S_{5b} are opposite. According to the analysis of Watson,[32] for an AX_3Y molecule of C_{3v} symmetry there are 12 harmonic, 38 cubic, and 102 quartic independent force constants in a symmetry coordinate representation. In Tables 7−9 only the independent constants are listed. The dependent ones can be obtained from these using the relationships reported by Thiel et al.[33] Ab initio spectroscopic constants are reported in Table 10 and compared with the experimental values. In the calculation of ω_i, ν_i, x_{ij}, and g_{ij} constants, Fermi resonances have not been considered since the experimental parameters are all free from anharmonic perturbations, including those of the $\upsilon_4 = 1$ and $\upsilon_2 = \upsilon_5 = 1$ states which have been derived taking explicitly into account the Fermi resonance between them.[4,11,13]

7. Results and Discussion

The spectroscopic constants for all the analyzed bands have been determined with good precision. The values of the corresponding parameters of (35,16) and (37,16), in Tables 2−4, and those of (35,18) and (37,18) in Table 2 are in very nice agreement. Owing to the small number of assigned transitions in $2\nu_3 - \nu_3$ the D_{JK} and D_K constants could not be determined and have been kept fixed to the corresponding values in the $\upsilon_3 = 1$ excited state. The D_J constant resulted to be 94% correlated with B in all fits. The $\nu_1 + \nu_2$ and $\nu_2 + \nu_3$ bands of (35,16) have been analyzed[1] from infrared spectra recorded at lower resolution, 0.04 cm^{-1}; the present results reproduce the previous ones with higher precision. Also the results of the $\nu_2 + \nu_3 - \nu_3$ hot band of (35,16) from a high-resolution spectrum[3] have been improved in our analysis because twice as many transitions have been assigned and more precise lower state parameters[8] have been used.

The origins of the $\nu_1 + \nu_2$ and $\nu_2 + \nu_3$ bands have been combined with those of the fundamentals,[3−5,8,11] to derive the x_{12} and x_{23} anharmonicity constants in Table 10, using the classical formula for the energy of a vibration level for a molecule with doubly degenerate vibrations[34]

$$G(v_1, v_2, v_3, \ldots) = \sum_i \omega_i\left(v_i + \frac{d_i}{2}\right) + \sum_i \sum_{k \geq i} x_{ki}\left(v_i + \frac{d_i}{2}\right)\left(v_k + \frac{d_k}{2}\right) + \sum_i \sum_{k \geq i} g_{ki} l_k l_i + \ldots \quad (3)$$

In this equation $d_i = 1$ or 2 depending whether i refers to a nondegenerate or to a doubly degenerate vibration. The l_i

TABLE 10: Comparison between Calculated and Experimental Spectroscopic Parameters of $FClO_3$ (cm^{-1})

	$F^{35}Cl^{16}O_3$		$F^{37}Cl^{16}O_3$		$F^{35}Cl^{18}O_3$		$F^{37}Cl^{18}O_3$	
parameter	calcd	exptl	calcd	exptl	calcd	exptl	calcd	exptl
ν_1	1074.5	1063.2436(9)[a]	1071.4	1060.19923(1)[b]	1021.7	1011.107141(8)[c]	1017.9	1007.487731(9)[c]
ν_2	730.3	716.809727(8)[d]	720.6	707.15971(1)[b]	721.7	708.235180(6)[c]	712.8	699.329799(8)[c]
ν_3	552.8	549.87956(8)[e]	552.0	549.18943(8)[e]	538.5	536.00058(7)[e]	537.4	534.96527(8)[e]
ν_4	1335.1	1317.25415(3)[a]	1319.4	1301.70739(3)[b]	1294.5	1277.3106(2)[f]	1278.6	1260.8563(1)[f]
ν_5	590.7	590.31499(1)[g]	587.6	587.20959(1)[g]	565.6	565.10304(1)[g]	562.7	562.24628(1)[g]
ν_6	405.8	405.60551(5)[h]	405.8	405.50974(3)[h]	390.6	390.54063(3)[h]	390.6	390.49838(3)[h]
ω_1	1089.8		1086.5		1035.7		1031.8	
ω_2	740.9		731.2		732.4		723.5	
ω_3	559.9		558.9		545.0		543.7	
ω_4	1357.6		1341.4		1315.1		1298.1	
ω_5	595.8		592.6		570.3		567.3	
ω_6	410.8		410.6		395.3		395.2	
x_{11}	−1.73	−2.75025(8)[i]	−1.69	−2.73019(8)[i]	−1.62	−2.48390(5)[i]	−1.58	−2.46570(4)[i]
x_{12}	−1.84	−2.70231(8)	−1.79	−2.59107(7)	−1.69	−2.57903(4)	−1.58	−2.46610(4)
x_{13}	−1.45	−2.118[e]	−1.42	−2.145[e]	−1.43	−2.002[e]	−1.39	−2.003[e]
x_{14}	−7.82		−7.76		−7.06		−7.00	
x_{15}	−1.30	−2.461(2)[j]	−1.29		−1.18		−1.17	
x_{16}	−1.06	−1.559(2)[j]	−1.04		−1.01		−1.00	−1.401(5)[i]
x_{22}	−1.49	−1.45102(2)[i]	−1.52	−1.47035(2)[i]	−1.59	−1.53561(3)[i]	−1.63	−1.56743(4)[i]
x_{23}	−3.55	−3.85578(9)	−3.48	−3.79549(9)	−3.36		−3.29	
x_{24}	−0.05		−0.07		−0.50		−1.15	
x_{25}	−2.00	−1.50983(6)[f]	−2.02	−2.21516(7)[b]	−2.66	−1.5845(2)[f]	−3.19	−1.7037(2)[f]
x_{26}	−2.96	−2.785(2)[j]	−2.98		−2.87		−2.89	
x_{33}	−0.47	−0.6820(1)[i]	−0.45	−0.6658(2)	−0.36	−0.5620(1)[i]	−0.34	−0.5371(1)[i]
x_{34}	−2.45		−2.43		−2.40		−2.38	
x_{35}	−0.54		−0.52		−0.47		−0.45	
x_{36}	−0.64	−0.889(2)[j]	−0.62		−0.50		−0.47	
x_{44}	−5.44		−5.29		−5.13		−4.99	
x_{45}	−2.50		−2.42		−2.01		−1.68	
x_{46}	−1.42	−2.03150(4)[i]	−1.39		−1.40		−1.36	
x_{55}	−0.16	−0.26842(4)[k]	−0.16	−0.26404(4)[k]	−0.15	−0.25744(4)[k]	−0.15	−0.25368(4)[k]
x_{56}	−0.24		−0.24		−0.21		−0.21	
x_{66}	−0.47	−0.4838[l]	−0.47	−0.4867[l]	−0.42	−0.4374[l]	−0.43	−0.4439[l]
g_{44}	2.86		2.75		2.75		2.65	
g_{45}	−0.15		−0.10		0.13		0.43	
g_{46}	0.36		0.36		0.32		0.33	
g_{55}	0.09	0.11368(4)[k]	0.09	0.11334(4)[k]	0.07	0.09651(4)[k]	0.07	0.09654(4)[k]
g_{56}	−0.17		−0.17		−0.16		−0.16	
g_{66}	0.50	0.4619[i]	0.50	0.4634[l]	0.45	0.4185[l]	0.46	0.4241[l]
$\alpha_1^A \times 10^4$	5.03	5.7380(3)[b]	5.01	5.731(3)[b]	4.24	4.79950(9)[f]	4.23	4.79854(9)[f]
$\alpha_1^B \times 10^4$	2.59	3.2496(8)[b]	2.54	3.1848(6)[b]	2.48	3.07924(5)[f]	2.41	3.00703(8)[f]
$\alpha_2^A \times 10^4$	0.39	0.6038(1)[b]	0.42	0.61(3)[b]	0.43	0.60617(7)[f]	0.45	0.6056(1)[f]
$\alpha_2^B \times 10^4$	5.15	4.82325(5)[b]	5.01	4.6424(6)[b]	5.06	4.87331(5)[f]	4.98	4.77417(7)[f]
$\alpha_3^A \times 10^4$	−0.06	0.287(3)[b]	−0.08	0.272(2)[b]	−0.10	0.213(2)[f]	−0.13	0.196(8)[f]
$\alpha_3^B \times 10^4$	−0.09	0.263(1)[b]	−0.03	0.304(1)[b]	−0.36	−0.046(1)[f]	−0.33	−0.034(1)[f]
$\alpha_4^A \times 10^4$	6.06	6.7419(7)[b]	5.94	6.71(3)[b]	5.29	4.772(4)[f]	5.18	4.836(4)[f]
$\alpha_4^B \times 10^4$	2.87	3.3792(3)[b]	2.83	3.3211(6)[b]	2.71	3.2554(9)[f]	2.67	3.1147(1)[f]
$\alpha_5^A \times 10^4$	0.72	1.23(4)[b]	0.76	1.28(3)[b]	0.32	0.7421(1)[f]	0.35	0.7811(8)[f]
$\alpha_5^B \times 10^4$	−0.06	0.3321(8)[b]	−0.04	0.3803(6)[b]	−0.17	0.13082(5)[f]	−0.15	0.16987(4)[f]
$\alpha_6^A \times 10^4$	−0.18	−0.07(4)[b]	−0.19	−0.08(3)[b]	0.13	0.212(1)[f]	0.13	0.208(9)[f]
$\alpha_6^B \times 10^4$	4.54	4.848(1)[b]	4.54	4.8529(6)[b]	3.93	4.2117(7)[f]	3.94	4.2180(6)[f]

[a] From ref 4. [b] From ref 11. [c] From ref 5. [d] From ref 3. [e] From ref 8. [f] From ref 13. [g] From ref 7. [h] From ref 9. [i] From ref 12. [j] From ref 1. [k] From ref 14. [l] From ref 10. Standard uncertainties (1σ) in parentheses refer to the least significant digits.

quantum number assumes the values $l_i = v_i, v_i - 2, v_i - 4, ...,$ 1 or 0 and for a nondegenerate vibration $l_i = 0$ and $g_{ki} = 0$.

In addition, the x_{23} values equal to −3.85595(4) and −3.79546(4) cm^{-1} for (35,16) and (37,16), respectively, have been determined from the $\nu_2 + \nu_3 - \nu_3$ origins. They overlap the corresponding values from the combination bands within 2σ. Contrary, the x_{33} value of (37,16), −0.6538(2) cm^{-1}, obtained from $2\nu_3 - \nu_3$, differs by more than 3σ from that derived from the $2\nu_3$ overtone,[12] −0.6777(1) cm^{-1}. The number of transitions assigned to $2\nu_3$, 50, and the standard deviation of the fit, 0.00030 cm^{-1}, are very close to those of $2\nu_3 - \nu_3$, so it is difficult to choose between the obtained values and their average is reported in Table 10.

The agreement between calculated and experimental spectroscopic parameters is, in general, quite good. All fundamentals are reproduced within 6%, with larger deviations concentrated in the ν_1, ν_2, and ν_4 modes and with an absolute maximum deviation of about 18 cm^{-1} for the ν_4. These deviations are somewhat larger than expected from the application of the CCSD(T) level of theory to molecules of similar size (see, e.g., SiF_4 in ref 35) and originate from the difficulties in describing electron correlation in the hypervalent Cl atom. Most inaccuracies are probably concentrated in the harmonic force field, since anharmonicity constants are calculated with a root-mean-square deviation, rmsd, of 0.55 cm^{-1}. On the other hand, rotation vibration

TABLE 11: Comparison between Calculated and Experimental Isotopic Shifts of the Spectroscopic Parameters of $FClO_3$ (cm^{-1})

	$\Delta(F^{35}Cl^{16}O_3 - F^{37}Cl^{16}O_3)$		$\Delta(F^{35}Cl^{18}O_3 - F^{37}Cl^{18}O_3)$		$\Delta(F^{35}Cl^{16}O_3 - F^{35}Cl^{18}O_3)$		$\Delta(F^{37}Cl^{16}O_3 - F^{37}Cl\ ^{18}O_3)$	
parameter	calcd	exptl	calcd	exptl	calcd	exptl	calcd	exptl
ν_1	3.1	3.0	3.8	3.6	52.8	52.1	53.5	52.7
ν_2	9.7	9.7	8.9	8.9	8.6	8.6	7.8	7.8
ν_3	0.8	0.7	1.1	1.0	14.3	13.9	14.6	14.2
ν_4	15.7	15.5	15.9	16.5	40.6	39.9	40.8	40.9
ν_5	3.1	3.1	2.9	2.9	25.1	25.2	24.9	25.0
ν_6	0.0	0.1	0.0	0.0	15.2	15.1	15.2	15.0
x_{11}	−0.04	−0.02	−0.04	−0.02	−0.11	−0.27	−0.11	−0.26
x_{12}	−0.05	−0.11	−0.11	−0.11	−0.15	−0.12	−0.21	−0.12
x_{13}	−0.03	0.03	−0.04	0.0	−0.02	−0.12	−0.03	−0.14
x_{22}	0.03	0.02	0.04	0.03	0.10	0.08	0.11	0.10
x_{23}	−0.07	−0.06						
x_{25}	0.02	0.7	0.5	0.12	0.7	0.07	1.17	−0.5
x_{33}	−0.02	−0.02	−0.02	−0.02	−0.11	−0.12	−0.11	−0.13
x_{55}	0.0	0.0	0.0	0.0	−0.01	−0.01	−0.01	−0.01
x_{66}	0.0	0.0	0.0	0.0	−0.05	−0.05	−0.04	−0.04
g_{55}	0.0	0.0	0.0	0.0	0.02	0.02	0.02	0.02
g_{66}	0.0	0.0	−0.01	−0.01	0.05	0.04	0.04	0.04
$\alpha_1^A \times 10^4$	0.02	0.0	0.01	0.0	0.79	0.94	0.78	0.93
$\alpha_1^B \times 10^4$	0.05	0.06	0.07	0.07	0.03	0.17	0.13	0.18
$\alpha_2^A \times 10^4$	−0.03	0.0	−0.02	0.0	−0.04	0.0	−0.03	0.0
$\alpha_2^B \times 10^4$	0.14	0.18	0.08	0.10	0.09	−0.05	0.03	−0.13
$\alpha_3^A \times 10^4$	0.02	0.02	0.03	0.02	0.04	0.07	0.05	0.08
$\alpha_3^B \times 10^4$	−0.06	−0.04	0.03	−0.01	0.27	0.31	0.30	0.034
$\alpha_4^A \times 10^4$	0.12	0.03	0.11	−0.06	0.77	1.97	0.76	1.87
$\alpha_4^B \times 10^4$	0.04	0.06	0.04	0.14	0.16	0.12	0.16	0.21
$\alpha_5^A \times 10^4$	−0.04	−0.05	−0.03	−0.04	0.40	0.49	0.41	0.50
$\alpha_5^B \times 10^4$	−0.02	−0.05	−0.02	−0.04	0.11	0.20	0.11	0.21
$\alpha_6^A \times 10^4$	0.01	0.01	0.0	0.0	−0.31	−0.28	−0.32	−0.29
$\alpha_6^B \times 10^4$	0.0	0.0	−0.01	−0.01	0.61	0.64	0.60	0.63

interaction constants are well-reproduced, with an rmsd of 0.43×10^{-4} cm^{-1}. Owing to residual errors in the theoretical values, the comparison between experimental and theoretical isotopic shifts of the spectroscopic parameters is more significant. The values for the $^{35}Cl \rightarrow {}^{37}Cl$ and $^{16}O \rightarrow {}^{18}O$ shifts are listed in Table 11, columns 2−5 and 6−9, respectively. The agreement is very good except the differences for the x_{25} anharmonicity constants and α_4^A ro−vibration parameters. As shown in Table 7, the harmonic force field parameters of the degenerate modes are very close to those previously determined.[6,15] Instead, significant differences have been observed for the off-diagonal terms of the nondegenerate modes. The Potential Energy Distribution (PED) analysis reveals that the ν_2 and ν_3 modes are due to strong mixing of the "umbrella" bending and Cl−F stretching, in agreement with previous analyses.[6,15]

8. Conclusions

The anharmonic ab initio force field for perchloryl fluoride, together with additional band analyses, aimed to obtain a complete experimental characterization of this molecule, are presented. Though some improvements are appropriate for the harmonic part, the agreement between calculated and available spectroscopic data is in general good, giving support to the overall accuracy of the force field and to its usefulness for further experimental studies.

Acknowledgment. E.C., L.F., and R.T. acknowledge the financial support from the Università di Bologna and the Ministero della Ricerca e della Università, PRIN "Trasferimenti di energia e di carica: dalle collisioni ai processi dissipativi".

Supporting Information Available: Nine files containing the lists of the assigned transitions in the $\nu_1 + \nu_2$, $\nu_2 + \nu_3$, $\nu_2 + \nu_3 - \nu_3$, and $2\nu_3 - \nu_3$ bands of the studied isotopologues of $FClO_3$, together with the corresponding (observed − calculated) values obtained using the parameters of Tables 2−4 are provided. This material is available free of charge via the Internet at http://pubs.acs.org.

References and Notes

(1) Burczyk, K.; Bürger, H. *J. Mol. Spectrosc.* **1986**, *118*, 288.
(2) Heldmann, C.; Dreizler, H. *Z. Naturforsch., A: Phys. Sci.* **1990**, *45*, 811.
(3) Burczyk, K.; Bürger, H.; Le Guennec, M.; Wlodarczak, G.; Demaison, J. *J. Mol. Spectrosc.* **1991**, *148*, 65.
(4) Burczyk, K.; Bürger, H.; Halonen, L. *J. Mol. Spectrosc.* **1993**, *159*, 265.
(5) Meguellati, F.; Graner, G.; Bürger, H.; Burczyk, K.; Müller, H. S. P.; Willner, H. *J. Mol. Spectrosc.* **1994**, *164*, 368.
(6) Müller, H. S. P.; Gerry, M. C. L. *J. Mol. Spectrosc.* **1996**, *175*, 120.
(7) Meguellati, F.; Graner, G.; Burczyk, K.; Bürger, H.; Pawelke, G.; Pracna, P. *J. Mol. Spectrosc.* **1997**, *184*, 371.
(8) Meguellati, F.; Graner, G.; Burczyk, K.; Bürger, H. *J. Mol. Spectrosc.* **1997**, *185*, 392.
(9) Graner, G.; Meguellati, F.; Ceausu, A.; Burczyk, K.; Pawelke, G.; Pracna, P. *J. Mol. Spectrosc.* **1999**, *197*, 76.
(10) Graner, G.; Burczyk, K. *J. Mol. Spectrosc.* **2001**, *208*, 51.
(11) Cané, E.; Fusina, L.; Burczyk, K. *J. Mol. Spectrosc.* **2006**, *239*, 146.
(12) Cané, E.; Fusina, L.; Pawelke, G.; Burczyk, K. *J. Mol. Spectrosc.* **2007**, *244*, 24.
(13) Cané, E.; Fusina, L.; Burczyk, K. *J. Mol. Spectrosc.* **2008**, *247*, 57.
(14) Cané, E.; Fusina, L.; Burczyk, K. *J. Mol. Spectrosc.*, in press.
(15) Christe, K. O.; Curtis, E. C.; Sawodny, W.; Härtner, H.; Fogarasi, G. *Spectrochim. Acta* **1981**, *37A*, 549.
(16) Demaison, J. *Mol. Phys.* **2007**, *105*, 3109.
(17) Sarka, K.; Graner, G. *J. Mol. Spectrosc.* **2000**, *199*, 245.

(18) Stanton, J. F.; Gauss, J.; Watts, J. D.; Szalay, P. G.; Bartlett, R. J., with contributions from Auer, A. A.; Bernholdt, D. B.; Christiansen, O.; Harding, M. E.; Heckert, M.; Heun, O.; Huber, C.; Jonsson, D.; Jusélius, J.; Lauderdale, W. J.; Metzroth, T.; Michauk, C.; O'Neill, V.; Price, D. R.; Ruud, K.; Schiffmann, F.; Varner, M. E.; Vázquez, J. and the integral packages MOLECULE (Almlöf, J.; Taylor, P. R.), PROPS (Taylor, P. R.), and ABACUS (Helgaker, T.; Jensen, H. J. Aa.; Jørgensen, P.; Olsen, J.). For the current version, see http://www.aces2.de.

(19) Møller, C.; Plesset, M. S. *Phys. Rev.* **1934**, *46*, 618.

(20) Raghavachari, K.; Trucks, G. W.; Pople, J. A.; Head-Gordon, M. *Chem. Phys. Lett.* **1989**, *157*, 479.

(21) Dunning, T. H., Jr. *J. Chem. Phys.* **1989**, *90*, 1007.

(22) (a) Woon, D. E.; Dunning, T. H., Jr. *J. Chem. Phys.* **1995**, *103*, 4572. (b) Dunning, T. H., Jr.; Peterson, K. A.; Wilson, K. A. *J. Chem. Phys.* **2001**, *114*, 9244.

(23) Peterson, K. A.; Dunning, T. H., Jr. *J. Chem. Phys.* **2002**, *117*, 10548.

(24) Gauss, J.; Stanton, J. F. *Chem. Phys. Lett.* **1997**, *276*, 70.

(25) Allen, W. D.; Császár, A. G. *J. Chem. Phys.* **1993**, *98*, 2983.

(26) East, A. L. L.; Allen, W. D.; Klippenstein, S. J. *J. Chem. Phys.* **1995**, *102*, 8506.

(27) Papousek, D.; Aliev, N. R. *Molecular Vibrational−Rotational Spectra*; Academia: Prague, Czech Republic, 1982.

(28) Gaw, J. F.; Willetts, A.; Green, W. H.; Handy, N. C. In *Advances in Molecular Vibrations and Collision Dynamics*; Bowman, J., Ed.; JAI Press: Greenwich, CT, 1990.

(29) INTDER2000 is a general program developed by Allen, W. D. and co-workers which performs various vibrational analyses and higher order nonlinear transformations among force field representations.

(30) Allen, W. D.; Császár, A. G.; Szalay, V.; Mills, I. M. *Mol. Phys.* **1996**, *89*, 1213.

(31) King, W. T.; Mills, I. M.; Crawford, B. *J. Chem. Phys.* **1957**, *27*, 455.

(32) Watson, J. K. G. *J. Mol. Spectrosc.* **1972**, *41*, 229.

(33) Thiel, W.; Yamaguchi, Y.; Schaefer, H. F. *J. Mol. Spectrosc.* **1988**, *132*, 193.

(34) Herzberg, G. *Molecular Spectra and Molecular Structure II, Infrared and Raman Spectra of Polyatomic Molecules*; Nostrand Reinhold Company: New York, 1945; p 210.

(35) Wang, X.-G.; Silbert, E. L., III.; Martin, J. M. L. *J. Chem. Phys.* **2000**, *112*, 1353.

JP806710Q